

High performance catalytic activity of pure and silver (Ag) doped TiO₂ nanoparticles by a novel microwave irradiation technique

R. Senthil Kumar¹ · B. Gnanavel²

Received: 5 September 2016 / Accepted: 7 November 2016 / Published online: 14 November 2016
© Springer Science+Business Media New York 2016

Abstract This work reports the pure and silver doped-titanium dioxide (Ag-TiO₂) nanoparticles prepared by a novel one step microwave irradiation method. The results from powder X-ray diffraction indicate that both pure and Ag-TiO₂ nanoparticles are in anatase phase. The measured average crystallite sizes were found to be around 31 and 21 nm respectively. Transmission electron microscope observations revealed a uniform size distribution of spherical particles. The UV absorption edges are estimated from the UV–Vis absorption spectra by using UV–visible absorption spectroscopy. The results prove that the UV radiation absorption of prepared nanoparticles is improved and the absorption edge shifted towards longer wavelength. The photocatalytic degradation of different dyes such as azo-Methyl Red, Congo Red, and Orange G were investigated by using pure and Ag-TiO₂ catalyst under UV light irradiation. The result showed that the photocatalytic property is significantly enhanced by doping silver. This is due to charge separation and charge transfer between electron and hole of the Ag-TiO₂ catalyst. The samples were further characterized by photoluminescence and Fourier Transform infrared spectra analysis. Moreover, the method is simple, cost effective and high yields compared with other methods.

1 Introduction

Semiconductor Photocatalysis has been intensively studied since it was first reported by Fujishima and Honda in 1972 [1]. The intensive research was initiated on the development of photocatalysts for environmental applications by Frank and Bard [2] who investigated the use of TiO₂ nanopowder for the decomposition of highly polluting cyanide ions in water. The dyes such as, azo-Methyl Red (MR), Congo Red (CR) and Orange G (OG)) are one of the most hazardous contaminants in aquatic environment. Therefore, azo reactive dyes are used extensively, in which one or several azo (–N = N–) groups associated with substituted aromatic structures. These dyes are used in industries like textiles, leather, paper, ceramics, and food-processing technologies. The released wastewater from these industries causes the carcinogenic and mutagenic diseases to human health and environment. In addition, these exhibit harmful effect on the colour in the receiving water bodies and environment. The efficient degradation of azo dyes has become a challenging task in recent years due to their toxicity and contamination. Metal oxide photocatalytic degradation of organic pollutants has received keen interest by research communities due to its usefulness in tackling environmental contaminants. Further, transition–metal oxide nanomaterials (SnO₂, ZnO, TiO₂ and WO₃) have been intensively studied by researchers because of their significant physical and chemical properties. These nanoparticles could have diverse potential applications in optical and electronic fields [3]. Compared with other metal oxide semiconductor photo catalysts, TiO₂ based photo catalysts have been studied drastically in recent years. TiO₂ has following advantages over others. These are non phototoxic, high redox ability, high efficiency, low cost, chemically inert, non toxic and eco friendly. It finds various applications in industries due to its non-toxicity, relative

✉ R. Senthil Kumar
stsenthil84@gmail.com

¹ Research and Development Centre, Bharathiar University, Coimbatore, Tamilnadu 641 046, India

² PG and Research Department of Physics, Chikkaiah Naicker College, Erode, Tamilnadu 638 004, India

abundance and resistance to corrosion. It exhibits remarkable properties such as hydrophilicity as well as antibacterial and self-cleaning activity. Because of its optical activity, TiO₂ is often used in photocatalytic decomposition and more recently as a photocatalyst for the reduction of CO₂ to methanol [4]. There are several techniques were adopted for synthesis of pure and modified TiO₂ such as, hydrothermal [5], electrochemical [6], microwave [7], sonochemical [8], chemical precipitation method [9] and sol–gel methods [10]. Among these methods, chemical precipitation method offers simple methodology, high control of surface area, phase structure and morphology. These parameters were very crucial for determine the photocatalytic activity of TiO₂. In addition, microwave method has sparked much interest due to their operation simplicity, effective, low-cost route to synthesis, less time consuming (about 10 min), and for large-scale production.

Nowadays, research community has focused to improve the electrocatalytic and photocatalytic activity of TiO₂ nanoparticles by doping various metal ions [11], non-metal ions [12, 13], and exposed reactive anatase [001] facet [14]. Among all the above mentioned materials, metal ions doped TiO₂ nanoparticles play an important role in the charge carrier trap. It allows light absorption in the visible range and enhances surface electron excitation by visible-light excited plasmon resonance. As a result, it improved photocatalytic activity of TiO₂. Recently, silver doped TiO₂ nanoparticles have shown improved photocatalytic activity compared with pure TiO₂. Besides, it was suggested that Ag doped TiO₂ improves charge transfer and charge pair separation efficiency [15]. Therefore, in the present work, it is aimed to synthesis and characterizes the pure and Ag doped TiO₂ nanoparticles by simple microwave irradiation method. The effect of Ag concentration on structural, morphological, optical and photocatalytic properties of TiO₂ nanoparticles have been discussed.

2 Experimental procedure

2.1 Synthesis of pure and Ag doped TiO₂ nanopowders

Titanium (iv) isopropoxide (TTIP) and silver nitrate were purchased from spectrochem India, Isopropanol was purchased from SRL India. azo-Methyl Red (MR), Congo Red (CR), Orange G (OG)) were supplied from Merck. Pure and Ag doped TiO₂ nanoparticles were prepared by chemical precipitation method. All chemicals were used as received without any further purification. In a typical synthesis, 5 ml of TTIP solution was diluted with 25 mL of isopropanol under the strong stirring by using magnetic stirrer. Different weight

percentage of AgNO₃ (3 and 5) was added in the above solution with continuous stirring at room temperature till a clear and homogeneous solution was obtained. Then Ammonium solution (NH₄OH– as a precipitation agent) was added drop wise under strong magnetic stirring until the pH was maintained at 8.0. When light yellow color precipitates were obtained. The precipitate was washed with absolute ethanol to remove the NH₄⁺ ions. The resulting precipitate was transferred into Teflon lined household microwave oven (2.45 GHz) with power up to 900 W and irradiated for 15 min. Pure TiO₂ nanopowders were prepared in a same procedure without use of silver source.

2.2 Characterization techniques

The prepared nanopowders were successfully characterized by the following techniques. The crystalline structure and average grain size was analyzed by powder X-ray diffraction (XRD) using Bruker diffractometer within the 2θ range of 10°–80° using Cu Kα as X-ray source ($k = 1.5406 \text{ \AA}$). The particle size and surface morphology was analyzed using transmission electron microscopy (TEM) on a Technai G20-stwin high resolution electron microscope (HRTEM) using an accelerating voltage of 200 kV. The optical transmittance of the nanopowders was recorded at room temperature by using Perkin Elmer UV/VIS/NIR Lambda 19 spectrophotometer in the wavelength range of 300–900 nm. Photoluminescence spectra of the samples were collected at room temperature by using Cary Eclipse (e102045776) Fluorescence spectrophotometer in the wavelength range of 400–800 nm with a Xe laser as an exciting source, and excitation wavelength of 350. The Fourier transformed infrared spectra (FT-IR) of the samples were collected using a 5DX FTIR spectrometer.

2.3 Photocatalytic experiment set up

The photocatalytic experiment on the prepared samples for the photodegradation of dyes is performed at ambient temperature. The photocatalytic activities of pure and Ag doped TiO₂ samples were evaluated by the degradation of three types of dyes, including azo-Methyl Red (MR), Congo Red (CR), Orange G (OG), in UV light radiation. For photocatalytic process, the dye solution was prepared by adding a particular concentration (for example 200 mL, $C_0 = 10 \text{ mg L}^{-1}$) and a particular amount of synthesized material poured into the dye solution. In the experimental set up, 250 ml of water cooled cylindrical glass reactor with 125 W high pressure UV lamp was used as a light source. The samples/dye solution was irradiated in the

horizontal direction and the distance between the UV lamp and the glass/dye solution was kept within 20 cm. Then the solution was kept in the dark room and well stirred with the magnetic stirrer for more than 30 min to attain the equilibrium condition throughout the solution. When the light was turned on, the experiment started. After a sudden irradiation time, the sample was taken out from the reactor. The concentration of the aqueous suspensions (phenol and methyl violet) in each sample was analyzed using UV–Vis spectrophotometer at a wavelength of 664 nm. The photocatalytic efficiency was calculated from the expression $\eta = (1 - C/C_0)$, where C_0 is the concentration of dyes (azo-Methyl Red (MR), Congo Red (CR), Orange G (OG)) before illumination and C is the concentration of dyes after a certain irradiation time. The time interval of irradiation time was maintained as 20 min.

3 Results and discussion

3.1 Powder X-ray diffraction (XRD) analysis

Figure 1 shows the powder XRD pattern of pure and Ag doped TiO₂ nanoparticles with different Ag concentrations. It showed anatase-phase TiO₂ with characteristic diffraction peaks of 2θ values at about 25.1(101), 38.8(004), 47.9(200), 54.2(105), 55.8(211), 62.8(204), 68.5(101), 70.2(220) and 76.5(215), respectively. The results are in good agreement with the already reported literature values [4]. Ag doping does not influence the crystalline structure of TiO₂, but the peak position is shifted to lower angle side and decreasing the intensity as compared to pure TiO₂. This result suggests that Ag ions are merely doped with the

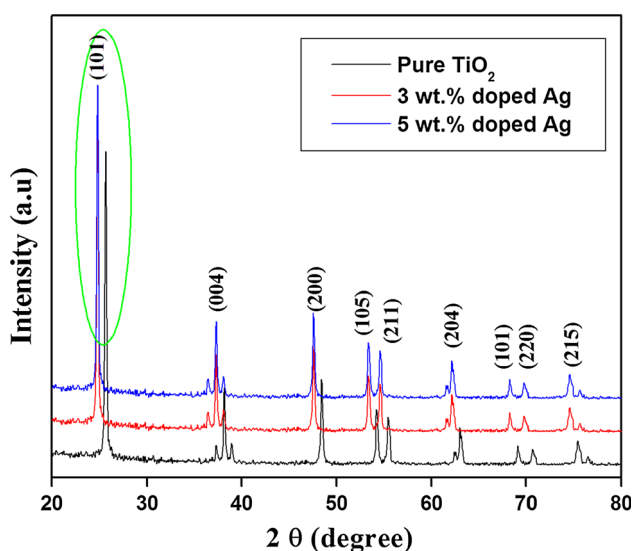


Fig. 1 Powder XRD pattern of TiO₂ nanoparticles with different Ag concentrations

surface of the crystal without being covalently secured into the TiO₂ host lattice. Furthermore the lattice parameters and average grain size of pure TiO₂ was reduced with increase in the Ag concentrations (see Table 1).

The average crystallite size can be determined through Full-width at Half Maximum (FWHM) of X-Ray diffraction peak by using Debye-Scherrer's equation [16].

$$d = \frac{K\lambda}{\beta \cos \theta}$$

Where d is the mean crystallite size, K is the shape factor taken as 0.89, λ is the wavelength of the incident beam, β is the full width at half maximum and θ is the Bragg angle. The calculated average crystalline size was 31, 26 and 21 nm for pure and Ag (3 and 5 wt%) doped TiO₂ respectively. The decrease in crystalline size or increase in the surface area due to Ag ions could be substituted in the regular lattice site of TiO₂ and the grain growth is arrested for pure TiO₂.

3.2 Transmission electron microscope analysis

TEM is a useful technique to determine the surface morphology and average particle size of the samples. Figure 2 shows the TEM images of pure and Ag doped TiO₂ nanoparticles. Both the samples show evidence of mostly spherical shaped morphology with agglomeration particle distribution. There is no considerable change in the morphology, but the average particle sizes were decreased from 32 to 18 nm for Ag doped samples. This result was good in agreement with the average crystalline size calculated from Debye-Scherrer's formula by XRD method.

3.3 UV–Vis transmission spectra analysis

Figure 3 shows the UV–Vis spectra pure and Ag doped TiO₂ nanoparticles. It was noted that the pure TiO₂ sample shows the strong UV absorption edge at 373 nm. With increase of Ag content, this absorption edge was increases and also shifted towards longer wavelength, which is a characteristic of surface plasma resonance.

The optical absorption coefficient (α) of a semiconductor is expressed by the following equation [17],

$$\alpha = A(h\nu - E_g)^n/h\nu$$

Where α is the absorption coefficient, h is the Planck's constant, ν is the frequency of incident light, E_g is the energy band gap of material and n is the factor governing the direct/indirect, etc. in the present case, for an indirect band gap, the value of n is $1/2$. The band gap energy was calculated as 3.15, 2.97 and 2.74 eV for pure and Ag (3 and 5 wt%) doped TiO₂ samples (Fig. 3b). The observed decrease in band gap energy can be attributed to the Ag ions can give rise to localized

Table 1 Shows the lattice parameters and crystallite size of TiO₂ nanoparticles with different Ag concentrations

Ag concentrations (wt%)	Crystallite size (nm)	Lattice parameters		Cell volume (Å ³)
		a (Å)	c (Å)	
0	31	3.7891	9.4874	136.21
3	26	3.6756	9.4321	127.42
5	21	3.6634	9.3241	125.13

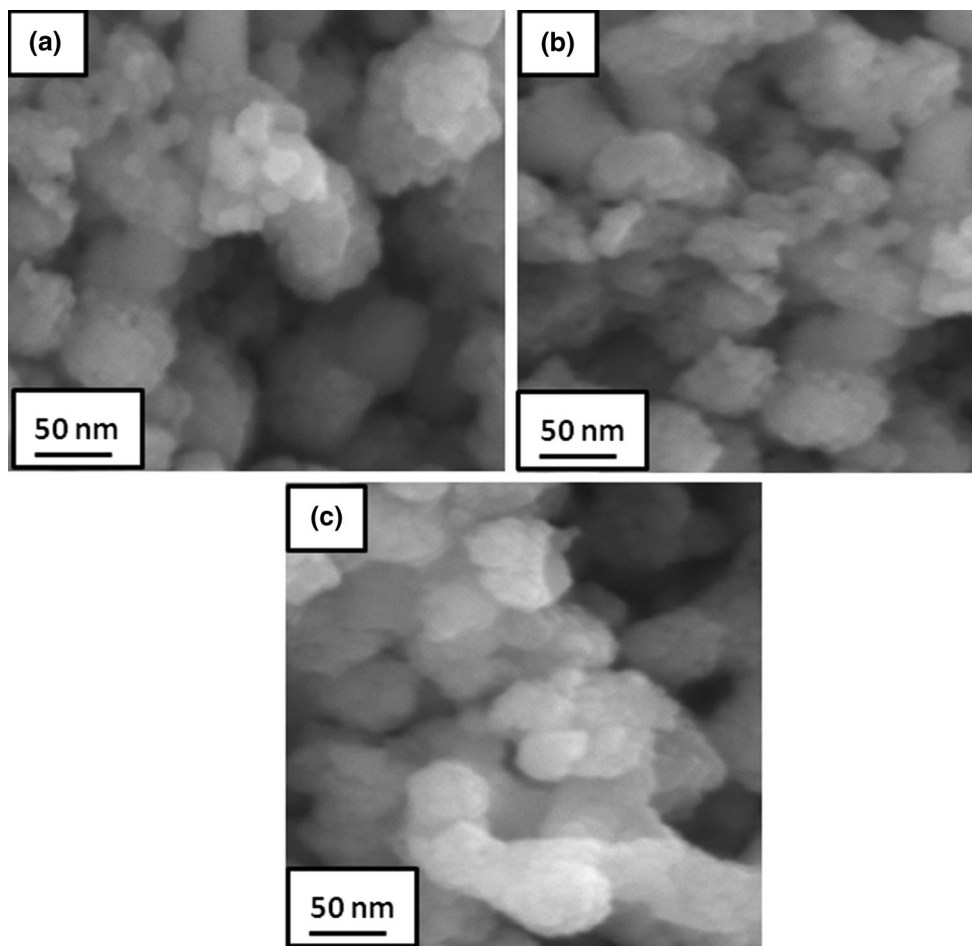


Fig. 2 TEM images of TiO₂ nanoparticles **a** pure TiO₂ **b** 3 wt% Ag **c** 5 wt% Ag

energy in the band gap of TiO₂ into which valence band electrons of TiO₂ are excited at wavelength longer than the absorbance edge., Wu et al. [18] reported that the narrowing of the band gap can improve the photocatalytic activity under visible light. This might explain our results for the photocatalytic activity of investigated samples.

3.4 Photoluminescence spectra analysis

Photoluminescence spectroscopy (PL) is a useful technique for probing the electronic structure of nanomaterials, the transfer behavior of the photoexcited electron–hole pairs in semiconductors, and the rate of recombination [19]. Figure 4 shows the PL emission spectra of both pure and Ag

doped TiO₂ samples measured from 300 to 600 nm using a 325 nm He–Cd laser. In pure samples, there are series of three emission peaks centered in all the samples at wavelengths of 362, 378, 412, 446, 491 and 523 nm, respectively. There is no change in the peak position but the intensity was increases with the increase of Ag doped samples. The UV emission peaks at 362 and 378 nm is considered as the band edge emission of the host TiO₂, and this can be ascribed to self-trapped excitations localized in TiO₆ octahedra [20]. The emission peak in a range of 400–470 nm, correspond to the radiative transition of the excited electrons from occupied d bands to higher states of the Fermi level. The existences of green emission peak at 523 nm explain the presence of oxygen vacancies [21].

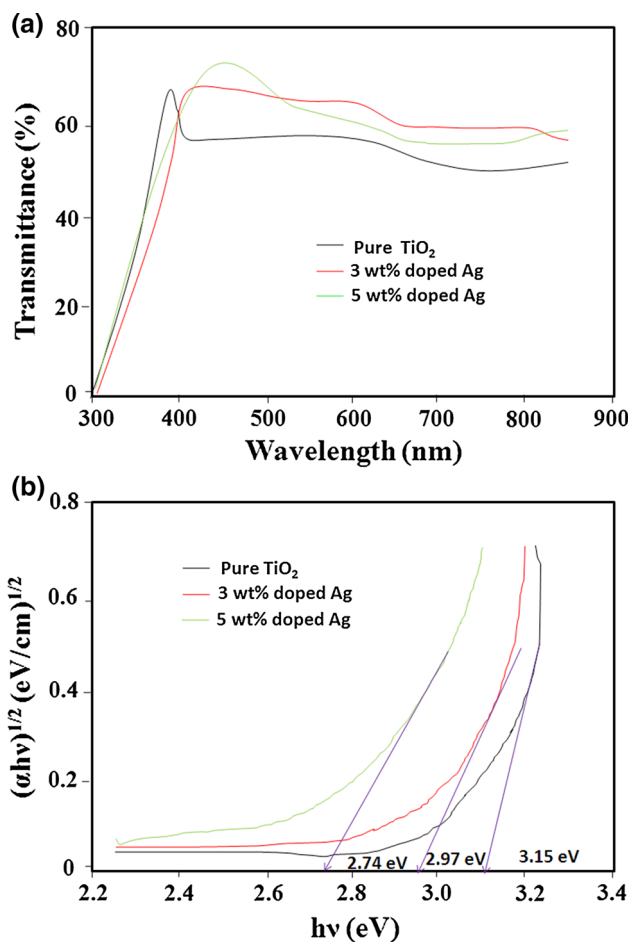


Fig. 3 UV-Vis spectra of TiO₂ nanoparticles with different Ag content **a** transmittance spectra **b** band gap energy plot

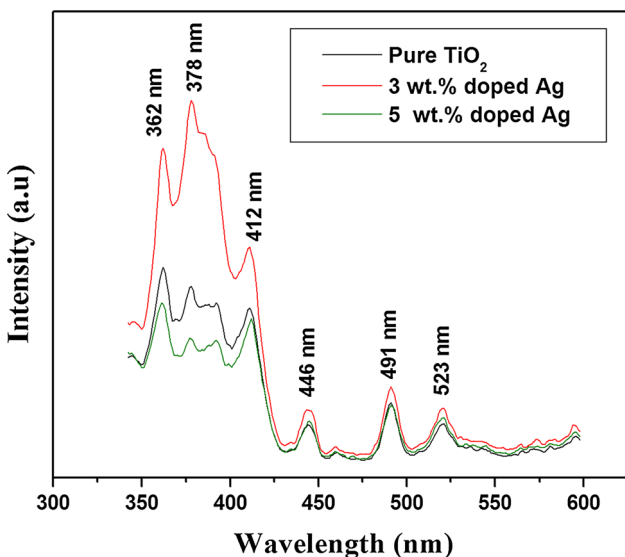


Fig. 4 Photoluminescence spectra of TiO₂ nanoparticles with different Ag concentrations

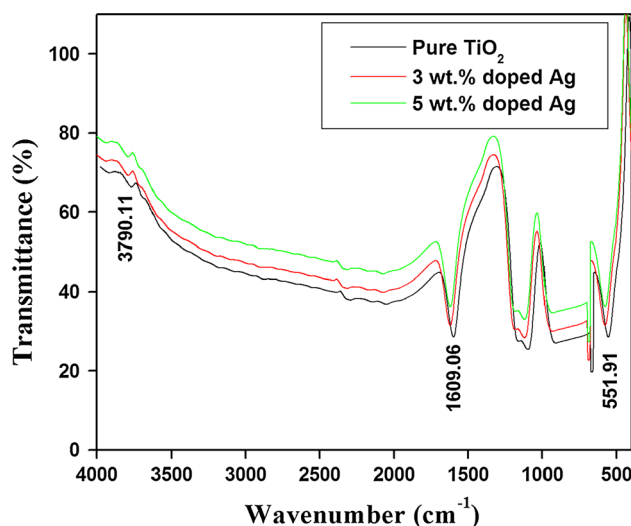


Fig. 5 FTIR spectra of TiO₂ nanoparticles with different Ag concentrations

Generally, the oxygen vacancies are present in three different charge states: V_o^0 , V_o^+ and V_o^{++} , in which V_o^0 is a very shallow donor. Among these, the 523 nm peak related to single oxygen vacancies (V_o^+).

3.5 Fourier transform infrared spectra analysis (FTIR)

An FTIR spectrum is a useful method to identify the various functional groups and metal-oxide (MO) bond present in the compound. Figure 5 shows FTIR spectra of pure and Ag doped TiO₂ nanoparticles in room temperature. The broad absorption band at 3790.11 cm⁻¹ arises due to the stretching mode of O–H group that reveals the existence of a small amount of water absorbed by the TiO₂ nanostructure [22]. The peaks appearing at 1609.06 cm⁻¹ were attributed to H–O–H bending vibration mode of physically observed water [23]. In both pure and doped samples showed the broad band in the range 400–800 cm⁻¹ according to literature sources [24] is due to the stretching vibration of the Ti–O–Ti vibrations. No other peaks related to Ag were observed, but the peak position is slightly shifted to lower wavenumber side. This reveals that Ag incorporation in the TiO₂ lattice site.

3.6 Photocatalytic studies

The photocatalytic activities of pure and Ag doped TiO₂ catalysts were investigated based on their ability to degradation of various dyes such as azo-Methyl Red (MR), Congo Red (CR), Orange G (OG)) under UV light irradiation. The photocatalytic degradation of TiO₂ with different Ag content were depict in Figs. 6, 7 and 8. It could be

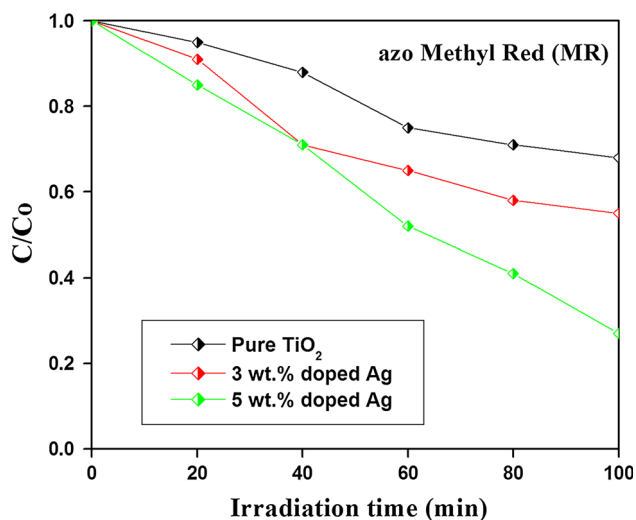


Fig. 6 Photocatalytic degradation of MR using Ag-TiO₂ catalyst under UV light irradiation

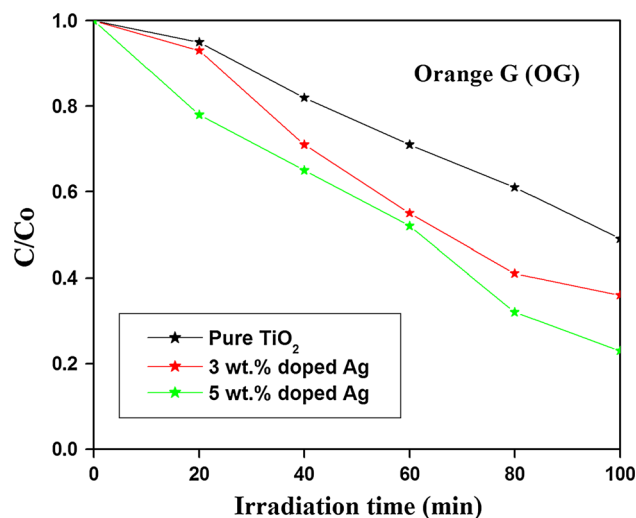


Fig. 8 Photocatalytic degradation of OG using Ag-TiO₂ catalyst under UV light irradiation

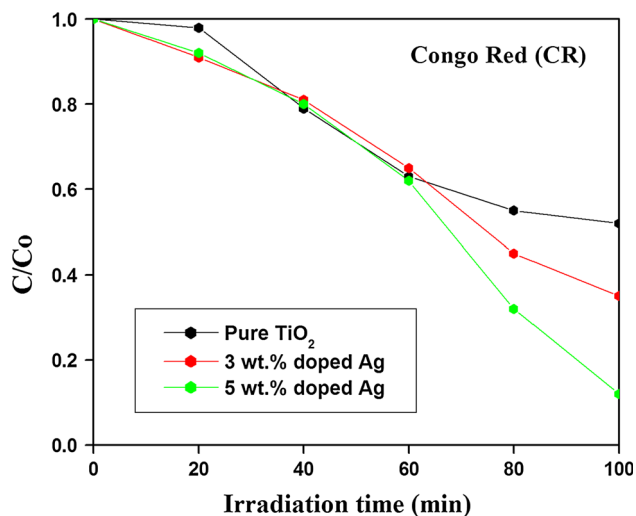


Fig. 7 Photocatalytic degradation of CR using Ag-TiO₂ catalyst under UV light irradiation

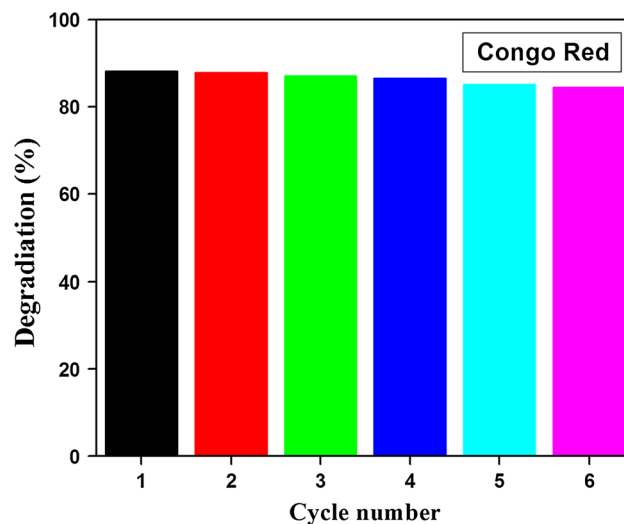


Fig. 9 Recycling cycles of test of CR using Ag-TiO₂ as the photocatalyst

seen that with Ag doping amount increasing from 0 to 5 wt%, the degradation rate of all the dyes increased, which indicated that Ag was doped into TiO₂ lattice and enhanced the photocatalytic activity. After 100 min of testing, the degradation efficiency of MR was found to be 32%, after increasing the Ag concentrations degradation efficiency was 45 and 73%. Introducing of small amount of dopant ion can retard possible electron–hole recombination thus leading to enhanced photocatalytic activity. Similarly CR degradation efficiency of pure and Ag (3 and 5 wt%) was 48, 65 and 88% and OG degradation efficiency of pure and Ag (3 and 5 wt%) was 51, 64 and 77% respectively. For the reuse test, the photocatalyst was recollected by centrifuged and redispersed in the fresh dye solution followed by testing of the photocatalytic activity adopted the

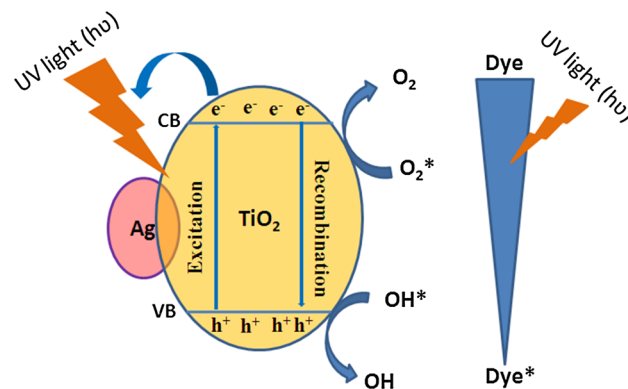


Fig. 10 Schematic representation for photocatalytic mechanism of Ag-TiO₂ catalyst

same procedure. The recycling test for Ag (5 wt%) doped TiO₂ catalysts in CR was shown in Fig. 9. The results show that Ag doped TiO₂ catalyst exhibits the excellent photocatalytic efficiencies of 88.2, 87.9, 87.1, 86.5, 85.1, 84.5% for 1–6 cycles. The slight variation in the photocatalytic degradation is due to the incomplete collection of the samples by the centrifugation process. Figure 10 schematically explains the photocatalytic mechanism of Ag-TiO₂ catalysts. When the presence UV light irradiation, The electron–hole pairs could be easily generated when the Ag-TiO₂, and then the generated electron–hole pairs reacted with water and molecular oxygen absorbed on the photocatalysis surface to form hydroxyl radicals ($\cdot\text{OH}$) and superoxide radical anions ($\cdot\text{O}^{2-}$) [25]. Ag also acted as a middle agent for the transfer of photo-generated electrons from the valence band of TiO₂ to an acceptor to produce superoxide radicals. Moreover, smaller band gap energy of Ag-TiO₂ catalysts (localized surface plasma resonance effect) was significantly enhanced photocatalytic effect. In addition, oxygen vacancy and high surface area of Ag on the surface of TiO₂ trap electrons and prevent the recombination of (e^- – h^+) pairs. This process could be a remarkable effect in the improvement of photocatalytic process.

4 Conclusions

In summary, pristine and Ag-doped TiO₂ nanoparticles were successfully synthesized by a novel one-step microwave irradiation method. XRD and TEM results confirm that the synthesized particles are anatase phase TiO₂ with crystalline nature. The grain size decreases with increasing Ag concentration. A considerable red shift and narrowed band gap of pure TiO₂ (from 3.15 to 2.74 eV of Ag 5 wt% doped TiO₂) was observed for Ag doped TiO₂. Furthermore, UV and PL results confirm that the optical absorption of TiO₂ was in visible region. FTIR results revealed that the various functional groups are presented in pure and Ag doped TiO₂ nanoparticles. The Ag-TiO₂ photocatalyst exhibits better photo catalytic activity and good stability towards the different dyes such as, MR, CR and OG. This could be attributed to the localized surface plasmon resonance effect, which is promoting the main

reason for the enhanced photocatalytic activity. As a result, the prepared Ag-TiO₂ catalyst shows significant stability and could be used as a recyclable photocatalyst.

References

1. A. Fujishima, K. Honda, *Nature* **238**, 37 (1972)
2. S.N. Frank, A.J. Bard, *J. Am. Chem. Soc.* **99**, 303 (1977)
3. A. Fujishima, T.N. Rao, D.A. Truk, *J. Photochem. Photobiol. C* **1**, 1–21 (2000)
4. S. Bagheri, D. Ramimoghadam, A.T. Yousefi, S.B.A. Hamid, *Int. J. Electrochem. Sci.* **10**, 3088–3097 (2015)
5. K. Nagaveni, M.S. Hegde, N. Ravishankar, G.N. Subbanna, G. Madras, *Langmuir ACS j. surf. colloids* **20**, 2900–2907 (2004)
6. Z. Miao, D. Xu, J. Ouyang, G. Guo, X. Zhao, Y. Tang, *Nano Lett.* **2**, 717–720 (2002)
7. K. Ding, Z. Miao, Z. Liu, Z. Zhang, B. Han, G. An, S. Miao, Y. Xie, *J. Am. Chem. Soc.* **129**, 6362–6363 (2007)
8. Y. Zhu, H. Li, Y. Koltypin, Y.R. Hacothen, A. Gedanken, *Chem. Commun.* **17**, 2616–2617 (2001)
9. M. Nazari, N. Ghasemi, H. Maddah, M.M. Motlagh, *J. Nanos-struct. Chem.* **4**, 99–103 (2014)
10. M. Zhang, Y. Bando, K. Wada, *J. mater. Sci Lett.* **20**, 167–170 (2001)
11. W. Choi, A. Termin, M.R. Hoffmann, *J. Phys. Chem.* **98**, 13669–13679 (1994)
12. Y. Choi, T. Umebayashi, M. Yoshikawa, *J. Mater. Sci.* **39**, 1837–1839 (2004)
13. J. Zhang, Y. Wu, M. Xing, S.A.K. Leghari, S. Sajjad, *Energy Environ. Science* **3**, 715 (2010)
14. B. Liu, H. Chen, C. Liu, S.C. Andrews, C. Hahn, P. Yang, *J. Am. Chem. Soc.* **135**, 9995–9998 (2013)
15. C. He, Y. Yu, X. Hu, A. Larbot, *Appl. Surf. Sci.* **200**, 2–10 (2002)
16. M. Parthibavarman, K. Vallalperuman, S. Sathishkumar, M. Durairaj, K. Thavamani, *J. Mater. Sci. Mater. Electron.* **25**, 730 (2014)
17. K. Gupta, R.P. Singh, A. Pandey, A. Pandey, *Beilstein J. Nanotechnol.* **4**, 345–351 (2013)
18. H.-C. Wu, S.-H. Li, S.-W. Lin, *Int. J. Photoenergy.* **7**, 115–119 (2005)
19. D.C. Hurum, A.G. Agrios, K.A. Gray, T. Rajh, M.C. Thurnauer, *J. Phys. Chem. B* **107**, 4545–4549 (2003)
20. W.Y. Wan, Y.M. Chang, J.M. Ting, *Cryst. Growth Des.* **10**, 1646–1651 (2010)
21. N.D. Abazovic, I.C. Mirjana, D.D. Miroslav, D.J. Jovanovic, A.S. Phillip, M.N. Jovan, *J Phys Chem B* **110**, 25366–25370 (2006)
22. T. Krishnakumar, R. Jayaprakash, M. Parthibavarman, A.R. Phani, V.N. Singh, *Mater. Lett.* **63**, 896–898 (2009)
23. B. Choudhury, A. Choudhury, *J. Lumin.* **132**, 178–184 (2012)
24. X.Z. Li, F.B. Li, *Environ. Sci. Technol.* **35**, 2381 (2001)
25. C. He, Y. Yu, *Appl. Surf. Sci.* **200**, 239–247 (2002)